This is the Pre-Published Version.

X. Chen, J. Zhou, X. Huang, S. Lu (2023) *Flame and burning dynamics of pool fire inside semi-confined compartment under external cross wind*, **Fire Safety Journal**, 103978. https://doi.org/10.1016/j.firesaf.2023.103978

Flame and burning dynamics of pool fire inside semi-confined compartment under external cross wind

Xiao Chen[a*], Jun Zhou[a], Xinyan Huang[b], Shouxiang Lu[a]

[a] State Key Laboratory of Fire Science, University of Science and Technology of China, Hefei, China

[b] Research Center for Fire Safety Engineering, Department of Building Environment and Energy Engineering, The Hong Kong Polytechnic University, Hong Kong, China

*Corresponding to summercx@ustc.edu.cn

Highlights:

- Three typical bending behavior of the tilted flame was observed inside semi-confined compartment.
- Air gap between the flame and sidewall was generated under the influence of cross wind.
- Nondimensional analysis of burning rate and cross wind explains flame height, tilted angle and air gap.

Abstract

In this paper, experimental and theoretical studies of the flame shape and burning rate of pool fire inside a semi-confined compartment (with one sidewall and ceiling open) under the cross wind were investigated. The effects of fuel pool size and cross wind velocity on the flame morphological parameters and burning rate were obtained. Three typical bending behavior of the tilted flame was observed during the experiments. The dimensionless burning rate $\dot{m}''^{*}$ decreased slightly when $Fr_w < 1$, and increased linearly with Fr_w when $Fr_w \geq 1$. An air gap (δ_{air}) between the flame and sidewall was observed because of the restriction of the sidewall and blow-off by strong airflow recirculation. Theoretical analysis of wind-blown pool fire inside the semi-confined compartment was conducted based on the asymmetrical air entrainment and the buoyancy length scale. A dimensionless parameter ($\frac{s\dot{m}_f}{\rho_\infty u_w {l_b}^2}$) considering the burning rate and cross wind velocity was proposed to predict the flame height, flame tilted angle and air gap thickness. The flame morphological characteristic parameters and the thickness of the air gap were correlated linearly well with the dimensionless parameter in exponent expression.

Keywords: Semi-confined compartment; Pool fire; Cross wind; Flame height; Thickness of air gap

1. Introduction

Fire safety of container cargo ships attracted much attention in recent years as it was frequently reported that cargos were ignited; and finally, the whole ship was burned down under the cross wind. The fire events, occurring in the sailing container cargo ships, were affected by the ambient wind and cargos [1]. Stacking cargos of containers on ships would form the different restricted structures, and semi-confined compartment was one of the typical restricted structures. Many works on confined compartment fires on the ships have been studied recently [2-3].

The flame geometries and burning rate of pool fires under the cross wind in open spaces have been investigated by many scholars since 1960s, and lots of meaningful results were proposed [4-9]. Many morphological characteristics were proposed to quantify the change of flame geometry, including tilt angle and flame height (length). Scholars have conducted tremendous experiments under various wind conditions in order to reveal the change of flame geometry. Thomas [4,5] obtained the correlations of flame length and flame tilt angle from the wind-blown wood crib fire. The empirical correlations were improved by Ferrero [6] based on the large-scale liquid pool fire experiments (1.5-6m in diameter). Oka [7] conducted experiments with a propane burner and proposed the correlations of flame height and flame tilt angle, which are the function of wind Froude number Fr_w and the dimensionless heat release rate $\dot{Q}^*$. In the work of Lin and Delichatsios [8], square gaseous burner with a dimension of 8,10,15 and 20cm was employed to investigate the influence of horizontal cross wind ranging from 0m/s to 6.0m/s. They found that the basic flame morphological characteristics like flame height and flame tilt angle were associated with the cross wind speed, the turbulent flame buoyancy and the air required for stoichiometric combustion. Recently Lei [9] raised the new correlations for five geometric characteristics by introducing the buoyancy length scale and integrating the mixture fraction equation, which were based on the large-scale wind-blown pool fire experiments with the combustion area from 50m^2 to 400m^2.

The mass burning rate was an important parameter to assess the severity of pool fires and attracted much attention [10-14]. Blinov and Khudiakov [10] pioneered a series of systematic experiments on the scale effect of pool fire under a quiescent environment, revealing that the variation of mass burning rate with pool fire scale experiences three stages, which corresponds to the dominant mechanisms of conduction, convection and radiation, respectively. However, the mass burning rate of pool fire was quite different once the wind was involved, as the change of flame geometry results in the change of heat feedback. Therefore, many studies were carried out to investigate the effect of wind on mass burning rate. In Blinov's work[10], it was found that the mass burning rate increased with an increase in cross wind speed. However, the experiment results conducted by Welker [11]and Apte [12] showed the different trend that mass burning rate decreases as the wind speed increase in a relatively small range. Ping [13] found that the burning rate

of pool fire in both steady stage and boilover stage showed a non-monotonic response to the cross wind speed, which firstly decreased and then increased with the cross wind velocity. Hu [14] carried out a set of experiments with the cross wind speed up to 4.5m/s, which indicated that there were several transitions for the burning rate with increase in wind speed for different size pool fires from 25 to 75cm. These transitions were discussed based on the change of controlling mechanisms of feedback.

Recently several researchers paid attention to the effect of sidewalls on the pool fire behaviors. On basis of the experimental investigation, Gao [15] concluded that the flame height increases with the decrease of fire-sidewall distance due to the confined effect of sidewall, which restricts the air entrainment. Tao [16] studied the flame height of jet flame with three sidewalls and developed a global model to estimate the air entrainment of jet flame. A series of experiments of heptane pool fire closing to the tunnel sidewall were conducted by Ji [17] in order to reveal the sidewall effect on the flame characteristics and burning rate. The coupling effects of the sidewall and the cross wind received several attentions in recent years. Chen[18] experimentally investigated the combining effect of sidewall height and cross air flow on the mass burning rate, flame height and flame tilt behavior of pool fire. New correlations were proposed to predict the flame height and flame tilt angle in relation to the coupling effect of sidewall and cross wind. Ding [19] studied the flame tilt transition of heptane pool fire in the compartment with fully opening at the top under the cross wind and obtained the empirical correlation of flame tilt angle. However, the coupling effect of sidewalls and cross wind on the pool fire need further research.

In this study, experimental and theoretical studies of the flame shape and burning rate of pool fire inside semi-confined compartment under the cross wind were investigated. The effects of fuel pool size and cross wind velocity on the flame morphological parameters and burning rate were conducted. Three typical bending behavior of the tilted flame as well as the air gap were observed during the experiments. Theoretical analysis of wind-blown pool fire inside semi-confined compartment was conducted. Moreover, a dimensionless parameter considering the burning rate and cross wind velocity was proposed to predict the average flame height, flame tilted angle and the thickness of air gap.

2. Experimental setup

The experiments were conducted in a compartment with three sidewalls (Fig. 1), that is a semi-confined compartment with windward wall and top fully opening. The size of all three sidewalls is $40cm \times 40cm$, and both the top and windward opening is $40cm \times 40cm$. The front sidewall is constructed with a 5mm thick toughened glass in order to observe the variation of flame geometry, the other sidewalls and the baseboard are 7.5mm thick fire-resistant boards made of plaster.

The cross wind is provided by a small-scale wind tunnel with a length of 3m and width of 0.6m, which can produce stable and uniform cross air flow ranging from 0 to 3m/s. The range of the Reynolds number in the wind tunnel was $0\sim1.2\times10^5$ and the air flow in the outlet was fully-developed turbulence. The semi-confined compartment was fixed in front of the wind tunnel outlet with 0.6m separation distance horizontally and at the center of wind tunnel vertically. The compartment supported by for u-shaped steel columns was 20 centimeters off the ground and the impact of boundary layer between the wind tunnel and the compartment was slight. There were four anemometers at the outlet of the wind tunnel to record the wind velocity. The results of four anemometers showed that the fluctuation range of wind speed was less than 5% and the velocity gradient of the flow field at the center of outlet where the compartment was placed was neglectable. Hence, the cross wind at the outlet of wind tunnel can be considered as stable.

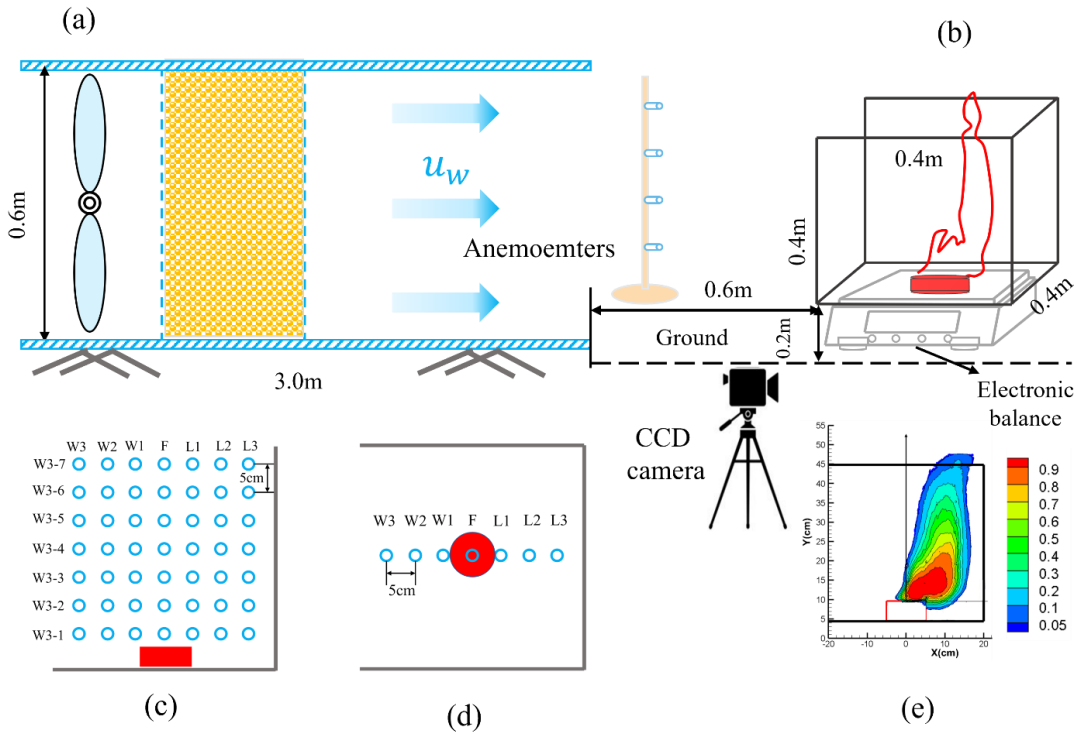

Fig. 1. Schematic diagram of experimental setup

The fuel pools employed in the experiments were made of 3mm thick stainless-steel plate with 4cm, 6cm, 8cm and 10cm in diameter. They were placed in the middle of the baseboard. Heptane was used as fuel and the liquid depth is 20mm at the beginning of each experiment. During the experiments, the depth of fuel decreased and no oil residue was found in the pan at the end of the experiments. Below the baseboard, an electronic balance with range of 6kg and accuracy of 0.01g was placed to record the mass loss of fuel. Seven thermocouple trees were set equally in the compartment with a distance of 5cm. Each thermocouple tree consists of seven thermocouples which are placed 5cm equally from the bottom to the top. The lowest

thermocouple is 5cm above the baseboard. The thermocouples were labelled as $W3, W2, W1, F, L1, L2, L3$ from the windward side to leeward side (as shown in Fig.1c). The influence of thermocouples on the air flow was considered to be slight since the diameter of thermocouple is only 1mm. A CCD camera (25fps) was positioned in front of the toughened glass to record the flame evolution. Forty-four experimental scenarios with different pool sizes and wind velocities were conducted, which are listed in Table 1.

Table 1. Experimental scenarios

Test No.	Fuel pool size (cm)	Cross wind velocity (m/s)
1-11	4	0, 0.21, 0.34, 0.6, 0.85, 1.06, 1.3, 1.71, 2.1, 2.6, 3.0
12-22	6	0, 0.21, 0.34, 0.6, 0.85, 1.06, 1.3, 1.71, 2.1, 2.6, 3.0
23-33	8	0, 0.21, 0.34, 0.6, 0.85, 1.06, 1.3, 1.71, 2.1, 2.6, 3.0
34-44	10	0, 0.21, 0.34, 0.6, 0.85, 1.06, 1.3, 1.71, 2.1, 2.6, 3.0

3. Results and discussions

3.1 Flame evolution and temperature field

Fig. 2 illustrates the flame evolution of the four pool fires of different scales inside semi-confined compartment under the cross wind velocity of 1.71 m/s. At the beginning, the flame area was small and the flame inclined to the leeward side due to the asymmetrical air entrainment. As the combustion progressed, the volume of flame and the flame height increased, the flame tilt became small because the buoyancy of plume increased. Finally, the flame body became smaller and the flame geometry was similar with the beginning. For the pool fire in larger diameter, the area of flame and the flame height are larger. When the flame is higher than the sidewall, the part of flame overflowing the semi-confined compartment will bend again owing to the inertial force of cross wind.

Fig. 3 and Fig. 4 depicts the flame geometry and the temperature field of pool fire inside the semi-confined compartment under the cross wind velocity ranged from 0 to 3m/s, respectively. With the increase of the cross wind velocity, the flame body becomes larger and the temperature of flame becomes higher. It can be observed in both Fig. 3 and Fig. 4 that the flame tilt and the area of flame base drag becomes larger with wind velocity increasing. When the cross wind velocity increases to a critical value, the tilted flame would bend before the flame tip touches the leeward sidewall due to the coupling effect of sidewalls and the crosswind. The flame extends vertically as the wind velocity continues to increase. When the flame overflows the semi-confined compartment, the second flame bending occurs.

Basing on the evolution process, three regimes of flame geometry can be recognized for the pool fire inside the semi-confined compartment under the cross wind: (a) tilted flame without bending; (b) tilted flame with once bending; (c) tilted flame with twice bending. The flame tends to overflow from top of the semi-confined compartment more easily when the pool size and the wind velocity is larger. Furthermore, it can be observed that an air gap exists between flame and the leeward sidewall in all three regimes. The combining effect of sidewalls and air entrainment forms a zone with high pressure which leads to an air flow between flame and the leeward sidewall. The intermittent fire whirl was observed during the experiments, which changed relatively smoothly. It indicated that the fire whirl reduced the turbulence of flame and suppressed the mixing of fuel and air, which may increase the flame height.

Fig. 2. Flame evolution of pool fire inside semi-confined compartment under the cross wind velocity of 1.71m/s

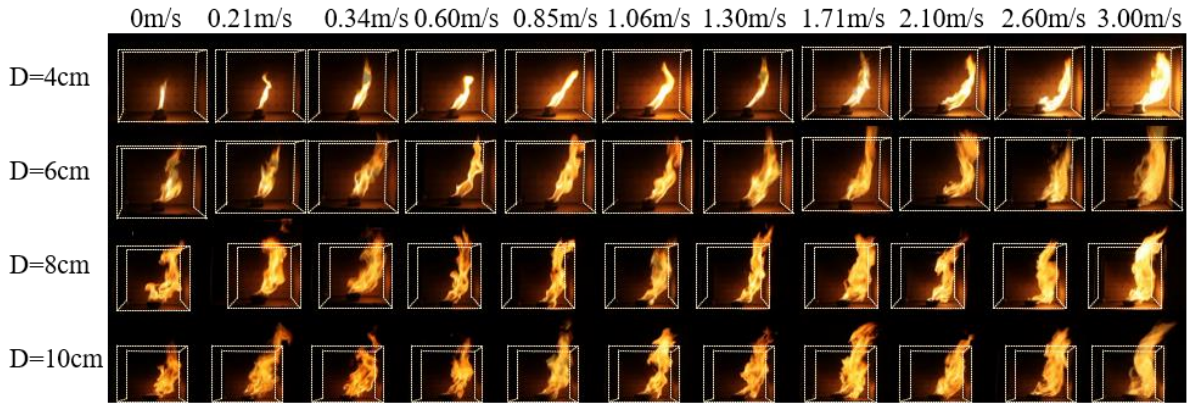

Fig. 3. Flame evolution of the different sizes of fuel pool in the steady burning stage with the cross wind velocity ranged from 0 to 3m/s

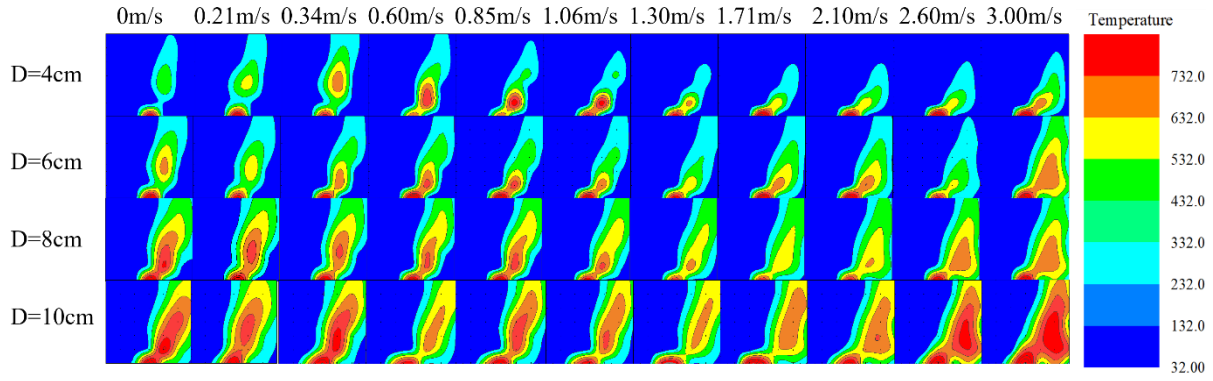

Fig. 4. Temperature field of pool fires inside semi-confined compartment with the cross wind velocity ranged from 0 to 3m/s

3.2 Mass burning rate

The mass burning rates of pool fires with different sizes of fuel pool under different cross wind velocities are illustrated in Fig. 5. In general, the three burning stages of the initial burning stage, fully developed burning stage and decay stage could be distinguished through the mass burning rate curves. From Fig. 5, the combusting duration of the pool fire under the relatively low wind velocity is longer than that under the relatively high wind velocity when the diameter of fuel pool is same. For Fig. 5(a) and (b), the maximum mass burning rate values of pool fires under strong wind are larger than which under weak cross wind. For Fig. 5 (c) and (d), the maximum mass burning rate value of pool fire under the cross wind velocity of 0.21m/s is larger than the pool fire under the cross wind velocity of 3.0m/s.

The average and maximum mass burning rate values of pool fires under different cross wind velocities are presented in Fig. 6. The average mass burning rate is calculated through the whole combustion period and the maximum mass burning rate corresponds to the peak value of the mass burning rate curve. The average mass burning rate shows a growing trend with the increasing cross wind velocity. The maximum mass burning rate the mass burning rate increases slightly first and then decreases followed by a steady increase as the wind velocity increases. Both the average and maximum mass burning rate values of pool fires with different source diameter are close when the cross wind velocity is 3m/s.

Blinov and Khudiakov [10] obtained an empirical correlation for the mass burning rate of wind-blown pool fire in open space basing on the experimental data of 0.3m to 1.3m diameter pool fire under the cross wind velocity ranging from 0 to 25m/s.

$$\dot{m}'' - \dot{m}_0'' = (\dot{m}_\infty'' - \dot{m}_0'')\left(1 - e^{-\beta u}\right) \quad (1)$$

where $\dot{m}_0''$ and $\dot{m}_\infty''$ are the mass burning rates under quiescent condition and the constant value with increasing wind velocity, and u is the cross wind velocity.

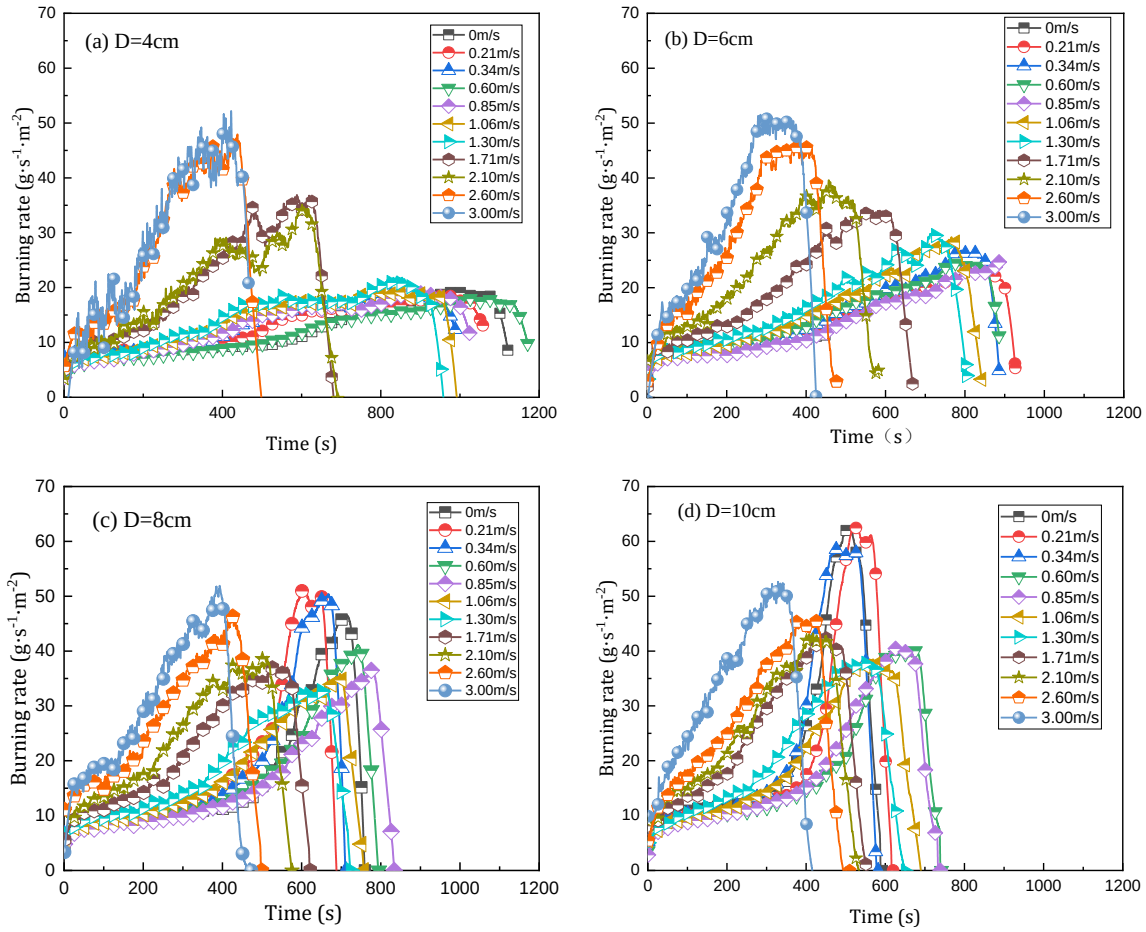

Fig. 5. Mass burning rates of the four sizes pool fire inside semi-confined compartment with the cross wind velocity ranged from 0 to 3m/s

Moreover, in the work of Blinov and Khudiakov [10], when the wind velocity is relatively small(0-3m/s), equation (1) can be changed as

$$\dot{m}'' - \dot{m}_0'' = (\dot{m}_\infty'' - \dot{m}_0'')\beta u \tag{2}$$

For the pool fire in the confined structure, the mass burning rate is affected by both the sidewall and the cross wind. Here we defined a new dimensionless parameter $\dot{m}''^{*} = \frac{\dot{m}''_{s,u\neq 0}}{\dot{m}''_{s,u=0}}$, where $\dot{m}''_{s,u\neq 0}$ is the mass burning rate of pool fire with sidewalls and cross wind and $\dot{m}''_{s,u=0}$ is the burning rate of pool fire in the confined structure under quiescent condition. The other dimensionless parameter $Fr_w{}' = u_w/\sqrt{g'D} =$

$\sqrt{\frac{T_\infty}{\Delta T_f}}Fr_w$ is introduced to describe the effect of cross wind and pool fire scale. As the flame temperature of different fuel is almost the same [20], the parameter Fr_w'can be simplified as Fr_w.

Fig. 7 depicts the relationship between $\dot{m}''^*$and Fr_w. $\dot{m}''^*$ decreases slightly and then increases with Fr_w and the critical value of Fr_w is about 1. Furthermore, $\dot{m}''^*$increases linearly with Fr_w when $Fr_w > 1$, which agrees with the result of Blinov and Khudiakov [10]. The critical wind Froude number ($Fr_w = 1$) means the buoyancy is competitive to the inertial force. When the wind Froude number is relatively small, the variation of mass burning rate with wind speed is complex because the flow field and the heat feedback is quite complicated. The effect of cross wind on heat feedback may be the domain mechanism and the mass burning rate increase linearly with the wind Froude number ($Fr_w = u_w/\sqrt{g'D}$) in relatively high wind speed.

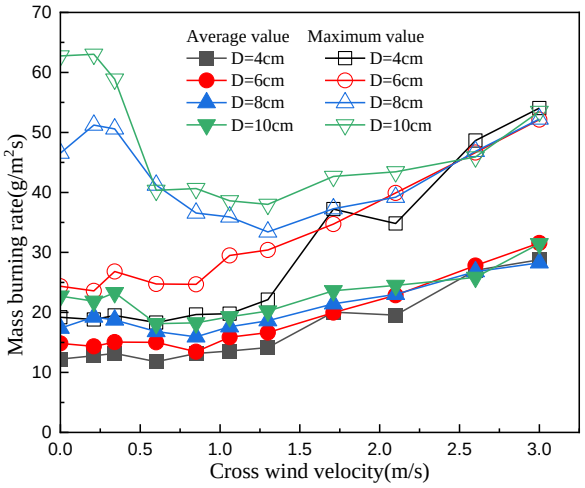

Fig. 6. Average and maximum mass burning rate values of pool fires under different cross wind velocities

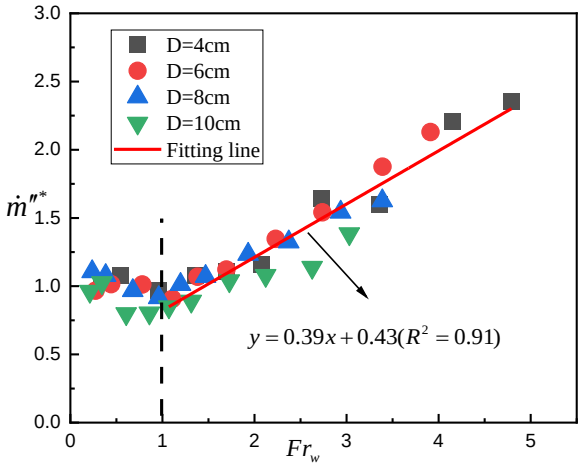

Fig. 7. The dimensionless mass burning rate ($\dot{m}''^*$)versus the Froude number (Fr_w)

3.3 Flame morphological characteristic parameters

3.3.1 Definition of flame morphological characteristic parameters

There are several flame geometric characteristics used to describe the evolution of flame like flame height and flame tilt angle. According to Fig. 3, three typical flame features distinguished from the flame images are illustrated in Fig. 8. The flame geometry depicted in Fig. 8(a) is similar to the fire plume in the open space with cross air flow when the source diameter and the wind speed are relatively small. When the

diameter of pool fire or the cross wind velocity increased, the flame would incline to leeward and bend in the flame bottom, like Fig. 8(b). When both the pool fire scale and the cross wind velocity are large enough and the flame overflow the semi-confined compartment, the flame geometry would be like Fig. 8(c). Based on Fig.8, several flame morphological characteristics are defined.

Two flame heights are defined by the contour of flame intermittency which is determined by Ostu[21] method. The average flame height $H_{f,aver}$ is calculated from the pool surface to the point of 0.5 intermittency. The maximum flame height is defined as the vertical length from the pool surface to the point of intermittency 0.05. The horizontal length L_x is defined as the horizontal distance from the center of fuel pool to the point of 0.5 intermittency for flame feature (a). For flame feature (b) and (c), L_x is measured from the center of fuel pool to the middle of the vertical part of flame. In addition, a transition point is defined as the point where the flame bends in the bottom of flame. The flame can be divided into three parts: (1) inclined part; (2) vertical part and (3) overflow part. Flame feature (b) is consisted with inclined part and vertical part. The position of transition point can be determined by the intersection of the central line of inclined part and vertical part (as shown in Fig. 8(b) and (c)). The flame tilt angle is defined as the angle between the central line of inclined part and the vertical direction. As can be observed in both Fig. 2 and Fig. 3, there is an air gap between flame and the leeward sidewall. The thickness of air gap δ_{air} is defined as the horizontal distance from the leeward sidewall to the flame outline where the intermittency is 0.05.

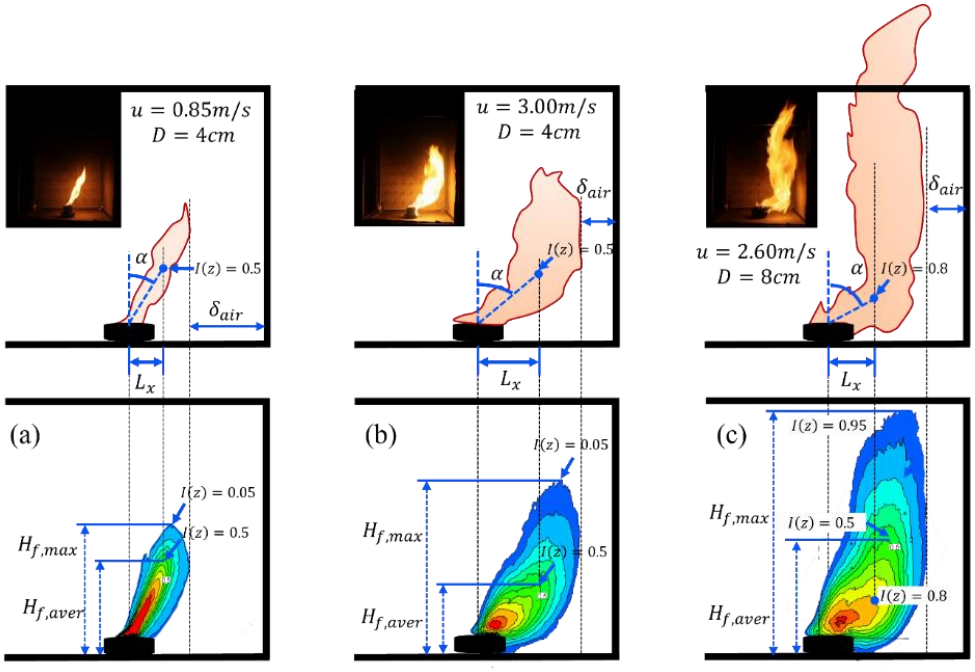

Fig. 8. Determination of flame morphological characteristics considering the effect of semi-confined compartment and the cross wind in the typical experimental condition.

3.3.2 Measured flame morphological characteristics

The average and maximum flame heights of four sizes pool fires inside semi-confined compartment under different cross wind velocities are presented in Fig. 9. In general, the average flame heights and the maximum flame heights of the pool fire with larger diameter are higher when the pool fire is under the same wind velocity. The variation of the maximum flame height with cross wind velocity is complicated as the flame heights of pool fires inside the semi-confined compartment are affected by many factors like mass burning rate and air entrainment.

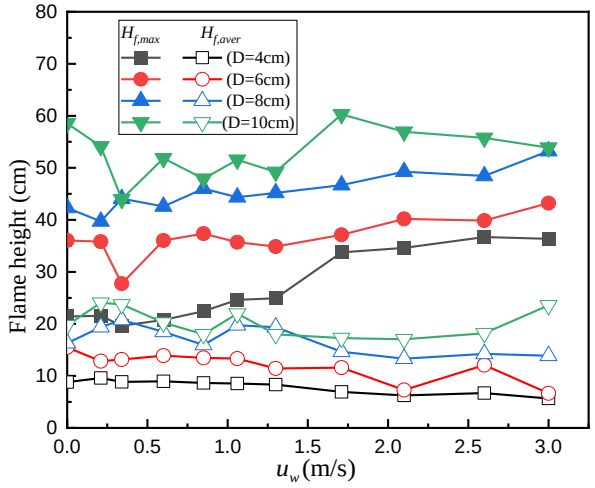

Fig. 9. The variation of the maximum flame heights and the average flame heights of different pool sizes in the semi-confined compartment with cross wind velocities

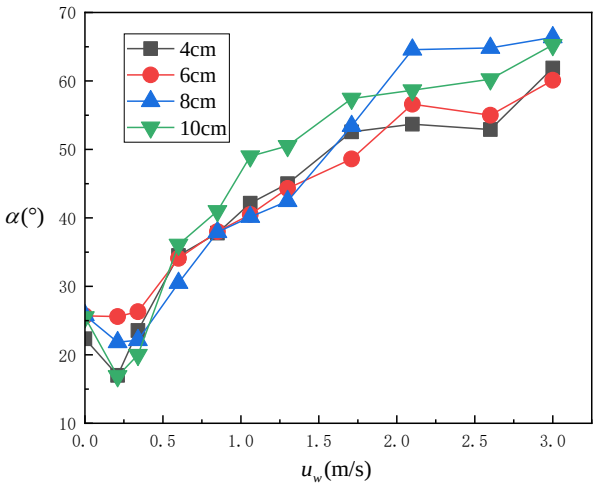

Fig. 10. The variation of the defined flame tilt angle α with the cross wind velocity u_w

The variation of the defined flame tilt angle α with the cross wind velocity u_w is shown in Fig. 10. The flame tilt angle α decreases slightly first and then increases and finally remains nearly unchanged as the wind speed increases. The variation is similar with the flame tilt angle of wind-blown pool fire in open space. However, the flame tilt angle without external cross air flow is larger than the flame tilt angle under the cross wind velocity of 0.21m/s due to the restricted air entrainment between flame and leeward sidewall.

The horizontal flame length L_x of pool fires with different wind speed is depicted in Fig. 11. The horizontal flame length of the pool fires with diameter of 4cm, 6cm and 8cm increases first and then fluctuate around a constant value as the cross wind velocity increases. However, the horizontal flame length decreases firstly, then increases and remains unchanged and goes down finally for 10cm diameter pool fire.

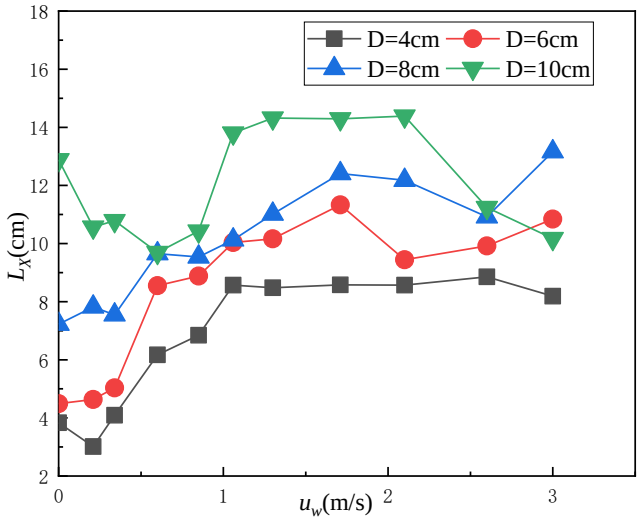

Fig. 11. Horizontal flame length L_x of different diameter pool fires inside semi-confined compartment under different wind velocities

Fig. 12 presents the variation of the thickness of air gap δ_{air} with the cross wind velocity. The thickness of air gap decreases first and then remains constant with wind speed increasing except when the diameter of pool fire is 10cm. It may be the distance between fire source and leeward sidewall caused the difference trend between 10 cm diameter case and the other cases. The influence of sidewall was more significant to the air entrainment with increase of pan diameter, which might change the flow field structure and the pressure distribution between fire source and leeward sidewall. The increase of δ_{air} for 10 cm diameter case is supposed to be caused by the flame rotation which will suppress the fuel diffusion and reduce the diameter of the rotating flame column.

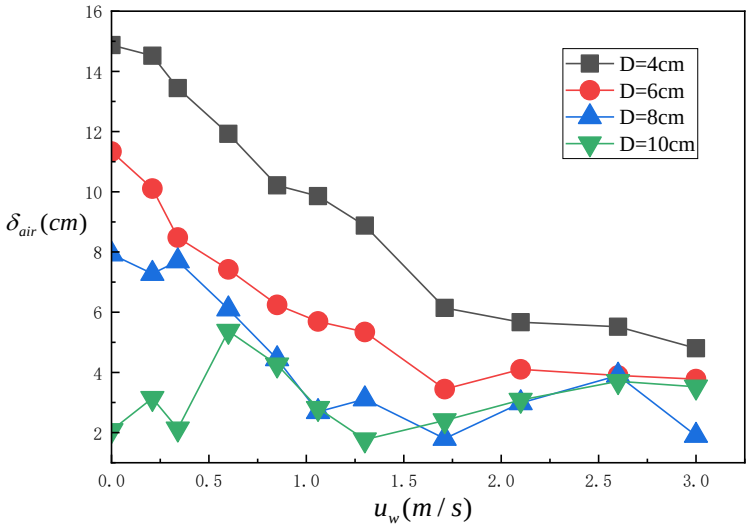

Fig. 12. The thickness of air gap δ_{air} of pool fires under different cross wind velocities

3.4 Theoretical analysis and correlations

Fig. 13 shows a physical model of the wind-blown pool fire inside semi-confined compartment. The flame geometry is determined by air entrainment and mixing of fuel and air, which are affected by the cross wind velocity, the sidewall and the heat release of pool fire.

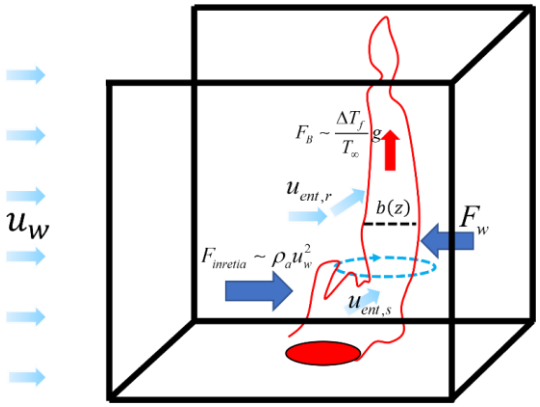

Fig. 13. A physical model for the flame geometry of pool fire inside semi-confined compartment under the horizontal wind

The physical model was developed based on the following assumptions:

(1) The combustion reaction is completely carried out on the flame surface, and the evaporated fuel and air react completely according to the stoichiometric ratio.

(2) The mass loss of the pool fire is negligible compared to the mass of entrained air.

(3) All the oxygen that entrained into the flame is consumed.

The air required for complete combustion is proportional to $s\dot{m}_f/\rho_\infty$, where $\dot{m}_f$ is the mass burning rate of pool fire, ρ_∞ is the density of air in the environment and s is the stoichiometric ratio which is according to fuel type. For heptane s is about 15.1. As the combustion of fuel is efficient and reaction occurred only on the flame surface, the flame geometric characteristics is decided by air entrainment. The mass rate of air entrainment can be integrated by the following equation:

$$\dot{m}_{ent} = \iint \rho_\infty u_{ent} dS \tag{3}$$

where u_{ent} is the velocity of air entrained into the flame surface. The vortex existed in the confined structure owing to the effect of sidewall and resulted in the occurrence of fire whirl. To simplify the analysis, we assume that the air entrainment of pool fire can be divided into two independent parts: the air entrainment induced by the vertical movement of flame and the air entrainment induced by the spinning of flame, and $u_{ent,r}$ and $u_{ent,s}$ are the rate of air entrainment, respectively.

$$\dot{m}_{ent} = \rho_\infty \int u_{ent,r} b(z) dz + \rho_\infty \int 2\pi b(z) u_{ent,s} dz \tag{4}$$

Under the cross wind condition, we assume $u_{ent,r} = a u_w$,$u_{ent,s} = k u_w$ and $b(z)$ is the half horizontal width of flame, a and k are the air entrainment coefficients.

$$\dot{m}_{ent} = \rho_\infty u_w \int_0^{H_f} b(z) dz + 2\pi \rho_\infty u_w \int_0^{H_f} b(z) dz = (a + 2\pi k) \rho_\infty u_w \int_0^{H_f} b(z) dz \tag{5}$$

$\int_0^{H_f} b(z) dz = \overline{b} H_f$, equation (5) can be simplified as:

$$\dot{m}_{ent} = K \rho_\infty u_w \overline{b} H_f \tag{6}$$

where K ($K = a + 2\pi k$) is the constant. The buoyancy length scale l_b ($l_b = \frac{F}{u_w^3}$,$F = \frac{g\dot{Q}}{\rho_\infty C_p T_\infty}$) is introduced to normalize the flame height which is used as the natural length scale of the pure plume under the action of wind [22].

$$\dot{m}_{ent} = K \rho_\infty u_w \overline{b} H_f = s\dot{m}_f \tag{7}$$

By dividing $\rho_\infty u_w {l_b}^2$ in both sides to normalize the mass of air required for complete combustion, the dimensionless formula below is obtained.

$$\frac{H_f}{l_b} \cdot \frac{\overline{b}}{l_b} = \frac{1}{K} \frac{s\dot{m}_f}{\rho_\infty u_w {l_b}^2} \tag{8}$$

Meanwhile, we can assume $\frac{H_f}{l_b} \cdot \frac{\overline{b}}{l_b} = \left(\frac{H_f}{l_b}\right)^{n+1}$ [23], and

$$\left(\frac{H_f}{l_b}\right)^{1+n} = \frac{1}{K} \frac{s\dot{m}_f}{\rho_\infty u_w {l_b}^2} \tag{9}$$

As Fig. 14 is shown, the experimental data of average flame height under the cross flow correlates well with the prediction model. The correlation is in the following:

$$\frac{H_f}{l_b} = 5.37 \left(\frac{s\dot{m}_f}{\rho_\infty u_w {l_b}^2}\right)^{0.54} \tag{10}$$

Change equation (10) to the form which is the function of the cross wind velocity and the mass burning rate as $H_f \sim \dot{Q}^{0.46} u_w^{-0.30}$. It means that the flame height increases with Q and decreases with the wind velocity.

On basis of the above analysis, other flame geometric characteristic length scale may have similar functional correlation with flame height.

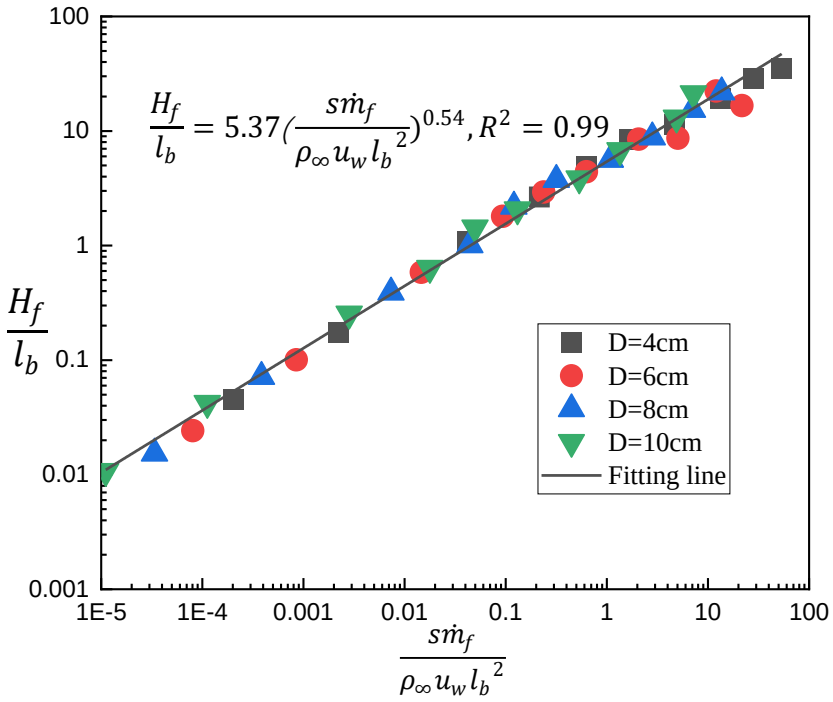

Fig. 14. Correlation for flame height of pool fire under the cross wind

The correlation of flame tilt angle and the horizontal flame length basing on the prediction model are depicted in Fig. 15 and Fig.16, which shows that both experimental data of the flame tilt angle and the horizontal flame length correlate well with the prediction model. And the correlation is followed:

$$\tan\alpha = 1.31(\frac{s\dot{m}_f}{\rho_\infty u_w {l_b}^2})^{0.12} \tag{11}$$

$$\frac{L_x}{l_b} = 4.46\left(\frac{s\dot{m}_f}{\rho_\infty u_w l_b^2}\right)^{0.63} \tag{12}$$

The potential variations of the flame tilt angle and the horizontal flame length with the mass burning rate and the cross wind velocity are written as $tan\,\alpha \sim \dot{Q}^{-0.12} u_w^{0.60}$ and $L_x \sim \dot{Q}^{0.37} u_w^{0.15}$.

However, for the thickness of air gap δ_{air}, it can be expressed as $\delta_{air} = L - L_x - b_{max}$,where L is the distance from the center of pool surface to the leeward sidewall and b_{max} is the maximum value of half horizontal width of flame.

Above all, we assume that $\frac{H_f}{l_b}\cdot\frac{\bar{b}}{l_b}=\left(\frac{H_f}{l_b}\right)^{n+1}$. The correlation of the flame height is obtained as equation (10), the value of n is calculated as 0.85. And the correlation of the average half horizontal width of flame could be indicated:

$$\frac{\bar{b}}{l_b}\sim\left(\frac{H_f}{l_b}\right)^{n}=fcn\left(\frac{s\dot{m}_f}{\rho_\infty u_w l_b^2}\right) \tag{13}$$

It is reasonable to assume $\frac{b_{max}}{l_b}=fcn\left(\frac{s\dot{m}_f}{\rho_\infty u_w l_b^2}\right)$.

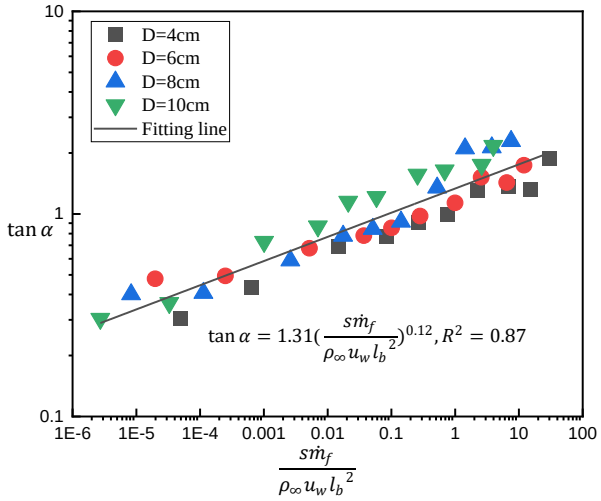

Fig. 15 Correlation for flame tilt angle of pool fire under the cross wind

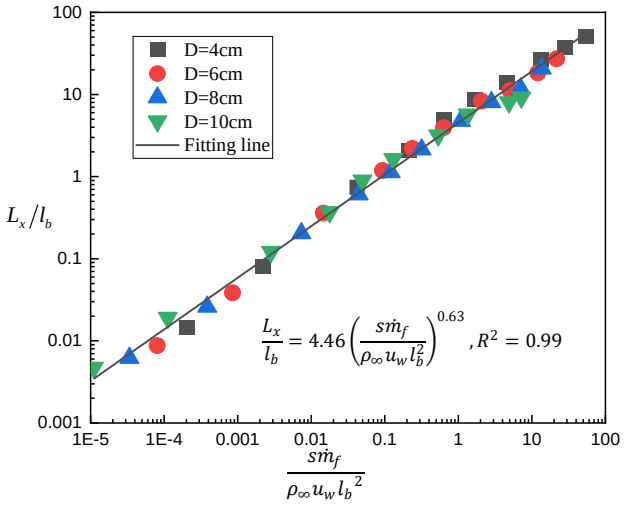

Fig. 16 Correlation for the horizontal flame length of pool fire under the cross wind

From equation (12), $\frac{L_x}{l_b}$ is also the function of $\frac{s\dot{m}_f}{\rho_\infty u_w l_b^2}$. As both $\frac{L_x}{l_b}$ and $\frac{b_{max}}{l_b}$ are the function of the characteristic parameter, we can deduce that

$$\frac{L-\delta_{air}}{l_b}=\frac{L_x+b_{max}}{l_b}=fcn\left(\frac{s\dot{m}_f}{\rho_\infty u_w l_b^2}\right)$$

In Fig. 17, the correlation is verified and it correlates well with the experimental data.

$$\frac{L-\delta_{air}}{l_b}=6.45\left(\frac{s\dot{m}_f}{\rho_\infty u_w l_b^2}\right)^{0.62} \tag{13}$$

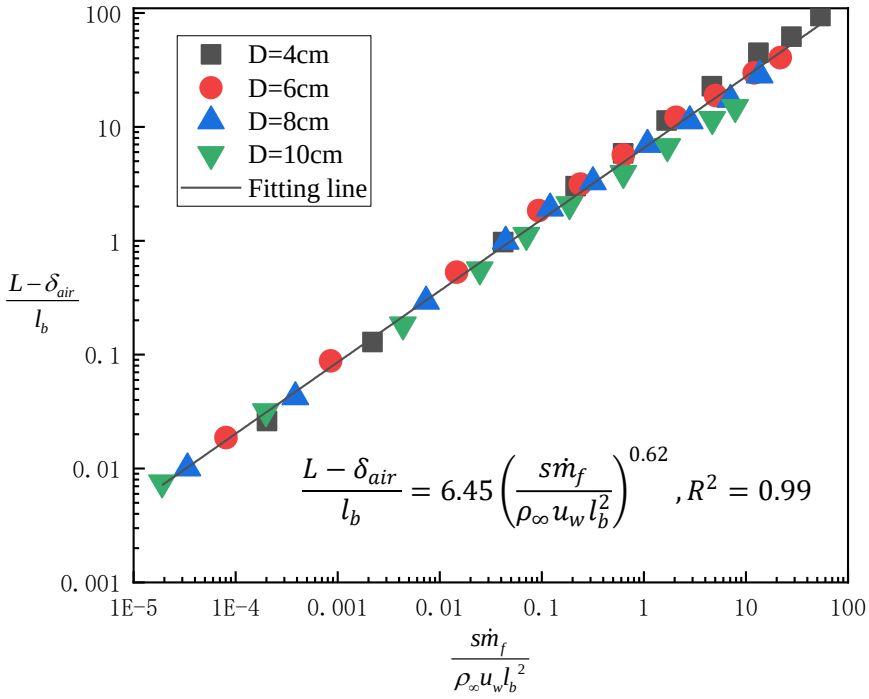

Fig. 17. Correlation for the air gap thickness

The correlations above are applicable when the following conditions are met.

(1) The cross wind is relatively strong and the applicability for low wind velocity cases needs to be validated in the future.
(2) The fire-sidewall distance is large enough that flame will not attach the sidewall.
(3) The flame length of overflow section is small. The correlations may fail when the average flame height is larger than the height of leeward sidewall because the rate of air entrainment cannot be calculated as Equation (4).

4. Conclusions

This paper experimentally and theoretically investigated flame and burning dynamics of pool fire inside a semi-confined compartment (with one sidewall and ceiling open) under the cross wind. The effects of fuel pool size and cross wind velocity on the flame morphological parameters and burning rate were studied. The major conclusions are listed as follows:

(1) Three typical bending behavior of the tilted flame was observed during the experiments: (a) tilted flame without bending; (b) tilted flame with once bending; (c) tilted flame with twice bending. An air gap between leeward sidewall and flame was found in all the tests due to the restriction of sidewall and the asymmetrical air entrainment.

(2) The average mass burning rate showed a growing trend with an increase of cross wind velocity in general. The dimensionless burning rate $\dot{m}''^{*}$decreases slightly when $Fr_w < 1$, and increased linearly with Fr_w when $Fr_w \geq 1$.

(3) A physical model for the pool fire inside a semi-confined compartment was constructed based on the theoretical analysis of the asymmetrical air entrainment. By introducing the buoyancy length scale l_b, a dimensionless parameter ($\frac{s\dot{m}_f}{\rho_\infty u_w {l_b}^2}$) considering the burning rate and the cross wind velocity was proposed to predict the flame height, flame tilted angle and the thickness of air gap. The flame morphological characteristic parameters and the thickness of air gap were correlated linearly well with the dimensionless parameter in exponent expression when the wind velocities are relatively high.

Acknowledgements

This work was supported by USTC Research Funds of the Double First-Class Initiative [grant number YD2320002008]; National Natural Science Foundation of China [grant number 51704268]; Fundamental Research Funds for the Central Universities [grant number. WK2320000044, WK2320000058].

References

[1] L.K. Wang, J.H. Wang, M.Y. Shi, S.S. Fu, M. Zhu, Critical risk factors in ship fire accidents, Marit. Policy Manag. 48 (6) (2021) 895-913, https://doi.org/10.1080/03088839.2020.1821110.

[2] Q. He, O. A. Ezekoye, C.H. Li, S.X. Lu, Ventilation limited extinction of fires in ceiling vented compartments. Int. J. Heat Mass Transf 91(2015) 570-583. https://doi.org/10.1016/j.ijheatmasstransfer.2015.07.080.

[3] X. Chen, S.X. Lu, Z.W. Ding, Initial fuel depth effect on the burning characteristics of thin-layer pool fire in a confined enclosure: Bench scale experiment and thermal equilibrium analysis. J Therm Anal Calorim 139 (2020) 1409-1418, https://doi.org/10.1007/s10973-019-08493-1.

[4] P.H. Thomas, R.W. Pickard, H.G. Wraight, On the size and orientation of buoyant diffusion flames and the effect of wind, Fire Saf. Sci. 516 (1963) -1–1.

[5] P.H. Thomas, Fire spread in wooden cribs: Part III the effect of wind, Fire Saf. Sci. 600 (1965) -1–1.

[6] F. Ferrero, M. Munoz, J. Arnaldos, Effects of thin-layer boilover on flame geometry and dynamics in large hydrocarbon pool fires, Fuel Process. Technol. 88 (3) (2007) 227–235,

[7] Y. Oka, O. Sugawa, T. Imamura, et al., Effect of cross-winds to apparent flame height and tilt angle from several kinds of fire source, Fire Saf. Sci. Proc.Seventh Int. Symp. 7 (2003) 915–926,

[8] Lin Y, Delichatsios M A, Zhang X, et al. Experimental study and physical analysis of flame geometry in pool fires under relatively strong cross flows[J]. Combust. Flame, 2019, 205: 422-433.

[9] J. Lei, W. Deng, S. Mao et al., Flame geometric characteristics of large-scale pool fires under controlled wind conditions, Proceedings of the Combustion Institute, https://doi.org/10.1016/j.proci.2022.07.132

[10] V.I. Blinov, G.N. Khudyakov, Diffusion Burning of Liquids, NTIS No. AD296762, U.S. Army Translation, 1961

[11] J.R. Welker, C.M. Sliepcevich, Burning rates and heat transfer from windblown flames, Fire Technol. 2 (3) (1966) 211–218, http://dx.doi.org/10.1007/bf02588554.

[12] V.B. Apte, A.R. Green, J.H. Kent, Pool fire plume flow in a large-scale wind tunnel. in: Fire Safety Science-Proceedings of the Third International Symposium, vol. 3, 1991, pp. 425–434, http://dx.doi.org/10.3801/iafss.fss.3-425.

[13] P. Ping, X. He, D. Kong, et al., An experimental investigation of burning rate and flame tilt of the boilover fire under cross air flows, Appl. Therm. Eng. 133 (2018)501–511, https://doi.org/10.1016/j.applthermaleng.2018.01.066.

[14] L. Hu, C. Kuang, X. Zhong, et al., An experimental study on burning rate and flame tilt of optical-thin heptane pool fires in cross flows, Proc. Combust. Inst.(2017), http://dx.doi.org/10.1016/j.proci.2016.08.021.

[15] Z.H. Gao, Z.X. Liu, J. Ji, et al., Experimental study of tunnel sidewall effect on flame characteristics and air entrainment factor of methanol pool fires, Appl. Therm. Eng. 102 (2016) 1314–1319, https://doi.org/10.1016/j. applthermaleng.2016.03.025.

[16] C.F. Tao, Y. Shen, R.W. Zong, et al., An experimental study of flame height and air entrainment of buoyancy-controlled jet flames with sidewalls, Fuel 183 (2016)164–169, https://doi.org/10.1016/j.fuel.2016.06.054.

[17] J. Ji, C.G. Fan, Y.Z. Li, et al., Experimental study of non-monotonous sidewall effect on flame characteristics and burning rate of n-heptane pool fires, Fuel 145 (2015)228–233, https://doi.org/10.1016/j.fuel.2014.12.085.

[18] Chen X, Ding Z, Lu S. Investigation of sidewall height effect on the burning rate and flame tilt characteristics of pool fire in cross wind[J]. Fire Safety Journal, 2021, 120: 103111

[19] Ding Z, Chen X, Lu S, et al. An investigation of flame tilt transition inside the compartment with horizontal opening in cross wind[J]. Proceedings of the Combustion Institute, 2021, 38(3): 4543-4550.

[20] Orloff L, De Ris J. Froude modeling of pool fires[J]. Symposium (International) on Combustion, 1982; 19(1): 885-895.

[21] Hoult D. P, and J. C. Weil. Turbulent plume in a laminar cross flow[J], Atmospheric Environment (1967), 6: 513-31. https://doi.org/10.1016/0004-6981(72)90069-8

[22] Otsu N. A threshold selection method from gray-level histograms[J]. IEEE transactions on systems, man, and cybernetics, 1979, 9(1): 62-66.

[23] J Fang, C. Jiang, J.W. Wang, J.F. Guan, Y.M. Zhang, J.J. Wang, Oscillation frequency of buoyant diffusion flame in cross-wind, Fuel 184 (2016)856- -863.